We are IntechOpen, the world's leading publisher of Open Access books
Built by scientists, for scientists

6,900
Open access books available

186,000
International authors and editors

200M
Downloads

154
Countries delivered to

Our authors are among the
TOP 1%
most cited scientists

12.2%
Contributors from top 500 universities

CLARIVATE ANALYTICS
BOOK CITATION INDEX
INDEXED

WEB OF SCIENCE™

Selection of our books indexed in the Book Citation Index
in Web of Science™ Core Collection (BKCI)

Interested in publishing with us?
Contact book.department@intechopen.com

7

Cable-based Robot Manipulators with Translational Degrees of Freedom

Saeed Behzadipour and Amir Khajepour

1. Introduction

Cable-based robots build upon mechanisms that not only use rigid links in their structures but also utilize unilateral force elements such as cables to deliver the desired motion. Cables may be either connected to active winches to provide a variable length and hence to actuate the mechanism or may be only to provide a kinematic constraint to eliminate an undesired motion of the end-effector. Manipulators in which the cables have variable lengths are usually called cable-driven or wire-driven manipulators.

Cable-based manipulators posses several advantages over conventional serial/parallel link manipulators including:

1. Large workspace: An active winch can provide a large range of length change on the cables at a low cost. This facilitates building manipulators for very large working spaces which cannot be obtained by other robots.

2. Low inertia: Materials provide their highest strength-to-mass ratio when they are under tensile loading. Using cables, which can be only in tension, maximizes the use of material strength and therefore reduces the mass and inertia of the manipulator. Low inertia is desirable in many applications including high speed/acceleration robotics.

3. Simplicity in structure: Cables simplify the robot structure by utilizing bending flexibility as kinematic joints and reducing the fabrication cost by minimizing the machining process.

4. Reconfigurability and transportability: Winch assemblies can be simply relocated to reconfigure and adjust the workspace of a cable-driven manipulator. The ease of assembly/disassembly of these manipulators also facilitates their transportation and quick setup.

5. Fully remote actuation: Using a fully cable-driven manipulator, all the actuators and sensitive parts are located away from the end-effector and the actual working area. Such manipulators best suit harsh or hazardous environments.

Open Access Database www.i-techonline.com

Source: Industrial-Robotics-Theory-Modelling-Control, ISBN 3-86611-285-8, pp. 964, ARS/plV, Germany, December 2006, Edited by: Sam Cubero

211

It should be also noted that using cable structures in robot manipulators is accompanied by theoretical and technical difficulties. The unilateral force of cables complicates the workspace, kinematics and dynamics analysis. The constraint of tensile force in all cables should be incorporated into the design and control procedure otherwise, the manipulator will collapse. Also, the low stiffness of the cables compared to rigid links may result in undesired vibrations requiring compensation by a proper control scheme.

As it was mentioned before, maintaining positive tension (tensile force) in all the cables is an essential requirement for the rigidity of a cable-based manipulator and hence, this property should be studied thoroughly before the cable-based manipulator can be used in any real application. In other words, a cable-based manipulator can be treated as a rigid link manipulator only if all the cables are in tension. As a result, most of the researchers' efforts on this category of robot manipulators have been spent on analyzing and proving the rigidity of the cable-based structures.

The general problem of rigidity in cable-based manipulators has been studied in the literature using different approaches and terminologies such as controllable workspace (Verhoeven & Hiller, 2000), dynamic workspace (Barette & Gosselin, 2005), wrench closure (Gouttefarde & Gosselin, 2006), manipulability (Gallina & Rosati 2002), fully constraint configuration (Roberts et al. 1998) and tensionability (Landsberger & Shanmugasundram, 1992). General formulation of this problem can be found in the works by (Ming & Higuchi 1994), (Tadokoro et al., 1996), and (Verhoeven et al., 1998). They showed that for the rigidity of a cable-based manipulator, it is necessary but not sufficient to have either actuation redundancy or separate external loading sources to produce tension in all cables. Ming (Ming & Higuchi 1994a,b) calls the first group Completely Restrained Positioning Mechanisms, CRPM, in which all the cables can be made taut with no external load while in an IRPM (Incompletely Restrained Positioning Mechanism), the manipulator cannot maintain its own rigidity and hence needs external load to make all cables taut.

The useful workspace of a cable-based manipulator is a subset of its geometrical workspace in which the manipulator can be rigidified (either by actuation redundancy or external loading). Determination of this workspace is the most essential step in the design and operation of a cable-based manipulator and is usually done by numerical search after the synthesis of the manipulator is done. Examples of this approach can be found in (Kawamura et al., 1995; Ferraresi, 2004; Ogahara, 2003; So-Ryeok et al., 2005a,b; Pusey et al., 2004). In this approach, if the workspace found through the search does not satisfy the design requirements, the synthesis of the manipulator and the workspace determination should be repeated. As a result and in order to avoid trial and error in the design, it is desired to have cable-based manipulators that can be rigidified everywhere in their geometrical workspace or at least their workspace can be analytically expressed. In this regard, a geometrical explanation for the

workspace of a cable crane has been found (Landsberger & Shanmugasundram, 1992) which is an IRPM. An analytical study for the boundaries of the workspace in planar cable-based manipulators is also performed in (Barette & Gosselin, 2005), (Gouttefarde & Gosselin, 2006) and (Stump & Kumar, 2006).

In this article, a series of cable-based manipulators with translational motion (Behzadipour, 2005) is studied with focus on their rigidity study. In these designs, cables are used to drive the end-effector as well as to eliminate its rotation by proper kinematic constraints. The significance of these new manipulators is that their rigidity can be guaranteed everywhere in their geometrical workspace by a certain set of conditions enforced on the geometry of the manipulator. This will be proved in details for each manipulator and the conditions will be derived. By incorporating these conditions into the design and control, the cables will be always taut and hence the cable-based manipulator can be treated as its rigid link counterpart.

In Section 2, the general structure of these manipulators will be presented and the critical concepts of rigidity and tensionability will be defined. In Section 3, a theorem is given to simplify the study of tensionability in these manipulators. In Sections 4 and 5, two spatial cable-based manipulators are introduced and their rigidity are proved. In Section 6, two planar manipulators with translational motion are presented and their rigidity are thoroughly studied.

2. General Structure and Definitions

The general configuration of the cable-based manipulators studied in this paper is shown in Fig. 1.

The four main elements of these manipulators are:

1. **Base**: The fixed part of the manipulator to which the global system of coordinate $OXYZ$ is attached

2. **End-effector**: The moving body which carries the moving frame $O'X'Y'Z'$.

3. **Cables**: The flexible tendon elements with negligible mass and diameter connected from one end to the end-effector at points P_i $(i=1,2,...,m)$ and pulled from the other end at Q_i. The pulling actuator produces tension τ_i inside the cable and can be simply a winch which pulls and winds the cable or a separate mechanism that moves the cable's end (Q_i) without changing its length. Unit vectors $\hat{\mathbf{u}}_i$ $(i=1,2,...,m)$ determine the direction of the cables and point towards the base. Depending on the structure of the manipulator, there may be some extra pulleys to guide the cables. The number of cables, m, is equal to the dimension of the motion space of the end-effector. Therefore, m is three and six for planar and spatial mechanisms, respectively.
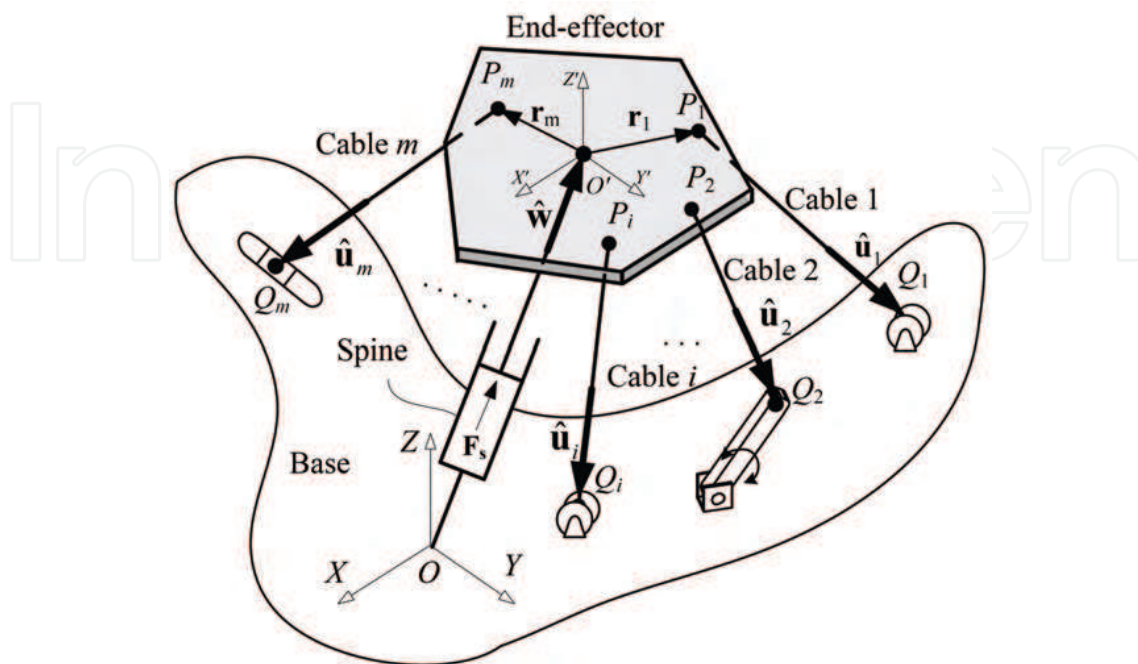
Figure 1. General configuration of the cable-based manipulators studied in this paper

4. **Spine**: The element that produces a force between the base and the end-effector in order to keep all the cables in tension. The spine can be an active element which generates a desired force. It can be also a passive element such as a cylinder energized by compressed air or a compressive spring designed properly to provide the sufficient force required to maintain tension in the cables. The direction of the spine is shown by unit vector $\hat{\mathbf{w}}$ pointing towards the end-effector.

For any cable-based manipulator, an equivalent rigid link counterpart can be found by replacing each cable by a rigid link and ball-and-socket joints at the ends. If the cable has a variable length, then a cylindrical element should be used to represent the cable in the rigid link manipulator. This analogy is valid as long as the cable-based manipulator is rigid according to the following definition:

Rigidity: A cable-based manipulator is rigid at a certain pose with respect to a given external load (including dynamic loads) and spine force if and only if all cables are in tension, $\tau_i \geq 0$ $i = 1,2,...,m$. A positive τ_i is considered as a tensile force in the cable.

It should be noted that the rigidity of a cable-based manipulator depends on the external load and therefore, dynamic forces should be also considered when the rigidity is evaluated. As a result, rigidity is not a property of the geometry only. The rigidity analysis requires the motion, inertia and all externally applied forces to be considered which complicates the process. To overcome this problem, another property called tensionability is defined and used which only depends on the geometry and expresses the potential of the manipulator for being rigid.

Tensionability: A cable-based manipulator is called tensionable at a given pose if and only if for any arbitrary external load there exists a finite spine force and a set of finite cable tensions to make the manipulator rigid.

Note that if a manipulator is tensionable and there is enough tensioning force available (by the spine and the cables), then the manipulator will be rigid under any external loading. In other words, tensionability and large enough tensioning force together provide a sufficient condition for the rigidity. The converse is that a manipulator may be rigid under a certain condition but not tensionable.

It is important to note that both rigidity and tensionability deal with the existence of the static equilibrium condition for the manipulator in which all the cables are in tension and hence, the manipulator does not collapse. However, they do not explain the nature of the equilibrium. Considering the stiffness of the manipulator, it may be rigid (meaning that it is in static equilibrium with all cables in tension) although the equilibrium might be an unstable one which implies that any small disturbance on the end-effector results in the collapse of the manipulator. It is known that the stability of the manipulator from the stiffness point of view is not specific to cable-based manipulators; however, it is shown in (Behzadipour & Khajepour, 2006) that the cable tensions may have a significant effect on the stiffness and even destabilization of the manipulator.

3. Tensionability

The goal of this section is to introduce an approach for the evaluation of tensionability in a cable-based manipulator. According to the definition, the tensionability of a manipulator must be evaluated for any arbitrary external load. In the following, a theorem is introduced which gives a sufficient condition for the manipulator to be tensionable.
The core idea of this theorem is to show that if positive tension (tensile force) can be generated in all the cables to any desired extent while the static equilib-

rium is satisfied in the absence of the external loads, then the manipulator can be rigidified under any arbitrary external load by having enough pretension in the cables.

Theorem 1.
A kinematically non-singular configuration of a cable-based manipulator is tensionable if for an arbitrary positive spine force $\mathbf{F}_s$ (compressive force), the static equilibrium equations of the manipulator have a solution with all positive cable tensions τ_i's.

$$\sum_i \tau_i \hat{\mathbf{u}}_i + \mathbf{F}_s = \mathbf{0} \tag{1}$$

$$\sum_i \mathbf{r}_i \times \tau_i \hat{\mathbf{u}}_i = \mathbf{0} \tag{2}$$

This theorem simply states that if the manipulator can stay rigid and statically balanced under an arbitrary compressive spine force, it is tensionable and thus can stay rigid for any external force and torque by choosing a large enough spine force.

Proof:
For the proof, it will be shown that such a manipulator can be made rigid for any arbitrary external load. The balance of forces for an arbitrary external force $\mathbf{F}_e$ applied at O' and moment $\mathbf{M}_e$ is:

$$\sum_i \tau_i \hat{\mathbf{u}}_i + \mathbf{F}_s + \mathbf{F}_e = \mathbf{0} \tag{3}$$

$$\sum_i \mathbf{r}_i \times \tau_i \hat{\mathbf{u}}_i + \mathbf{M}_e = \mathbf{0} \tag{4}$$

The above equations have a set of nontrivial solutions for τ_i's since the manipulator is assumed to be kinematically non-singular. Since the above set of equations is linear w.r.t. τ_i's, superposition can be applied to obtain the following two sets of equations:

$$\sum_i \tau_i^e \hat{\mathbf{u}}_i = -\mathbf{F}_e, \qquad \sum_i \mathbf{r}_i \times \tau_i^e \hat{\mathbf{u}}_i = -\mathbf{M}_e \tag{5}$$

$$\sum_i \tau_i^s \hat{\mathbf{u}}_i = -\mathbf{F}_s, \qquad \sum_i \mathbf{r}_i \times \tau_i^s \hat{\mathbf{u}}_i = \mathbf{0} \tag{6}$$

where $\tau_i^s + \tau_i^e = \tau_i$ for $i=1,2,...,m$. In this formulation, τ_i^s's are the cable forces to balance the spine force and are positive due to the assumption and τ_i^e's are the forces in the cables (positive or negative) due to the external force $\mathbf{F}_e$ and moment $\mathbf{M}_e$. If all τ_i^e's are positive, then τ_i's will be positive too and the cable-based manipulator is rigid. Otherwise, let $-\alpha^2 = \min_i(\tau_i^e)$ i.e. the most negative tension in the cables produced by the external load. Using the linearity of the static equilibrium equations in Eq. (6), cable tensions τ_i^s's can be increased by increasing f_s such that $\min_i(\tau_i^s) > \alpha^2$. As a result we have:

$$\min_i(\tau_i) \geq \min_i(\tau_i^s) + \min_i(\tau_i^e) > 0 \qquad (7)$$

Therefore, by increasing the spine force, the rigidity can be obtained and hence, the manipulator is tensionable.

The above theorem gives a sufficient condition for tensionability meaning that there might be situations in which the spine force cannot produce tension in all cables but the manipulator can be still rigidified. In those cases, sources other than spine may be used to generate tension in cables. An example of such cases will be studied in Section 5.1.

As a result from theorem 1, to evaluate the tensionability, instead of dealing with external load on the end-effector, we only need to show that the static equilibrium of the end-effector for an arbitrary spine force can be obtained by tensile forces in all of the cables. This will ensure that the manipulator is tensionable and thus can theoretically stand any external force and moment at the end-effector. By "theoretically" we mean that the required spine force and cable tensions are finite, although these forces may not be feasible due to the practical constraints. The above approach is used later in this paper to evaluate the tensionability of the new cable-based manipulators.

In the rest of this paper, some new designs of reduced DoF[1] cable-based manipulators are introduced. The target application of these manipulators is high-speed pick-and-place operations in which, small objects (less than 1kg) are moved with high speeds (more than 100 cycles per minute). High speed and acceleration requires low inertia which makes cable-based manipulators potential designs. However, most of the current spatial cable-based manipulators have 6 DoF while in pick-and-place applications, three translational axes of motion with a possible rotational DoF for reorienting the object are sufficient. In the designs presented in this work, cables are used to constrain the rotational motion of the end-effector in order to provide a pure translational mo-

---

[1] DoF: Degree of Freedom

tion. A more complete set of these designs can be found in (Khajepour et al., 2003). One of these designs, *DeltaBot*, has been prototyped at the University of Waterloo (Dekker et al. 2006). It can perform up to 150 cycles/minute of standard pick-and-place on small objects (less than 500gr).

4. BetaBot

In *BetaBot*, shown in Fig. 2, the upper triangle is the end-effector and the bottom one is the base. Three pairs of parallel cables are attached to the end-effector and wound by three winches after passing through guide holes on the winch frames. The winches are attached to the base. Each pair of cables forms a parallelogram such as *ABCD* as shown in the same figure. It is known that (Clavel, 1991), three parallelograms can eliminate the rotational motion of the end-effector. The spine is connected to the end-effector and base using two ball-and-sockets or one universal joint and one ball-and-socket. Therefore, the spine imposes no kinematic constraint on the end-effector.

The equivalent rigid link manipulator for *BetaBot* is obtained by replacing each cable with a slider with two ball-and-sockets at the ends. In this equivalent manipulator, there are 13 bodies, 12 ball-and-socket and 6 prismatic joints. The Gruebler equation gives $13 \times 6 - 12 \times 3 - 6 \times 5 = 12$ degrees of freedom. There are 6 trivial DoF's due to the twist of the sliders and there is also one constraint on each pair of sliders which forces their displacements to be the same (because each pair of cables is wound using a single winch). Therefore, the end-effector has $12 - 6 - 3 = 3$ DoF's which are translational.

Since the size of the end-effector plays no role in the kinematics of *BetaBot*, the end-effector can be shrunk to a point with three winches moving towards the center of the base accordingly. As a result, the kinematics of *BetaBot* becomes identical to that of a tripod (Mianowski & Nazarczuk, 1990), or the Tsai manipulator (Tsai, 1996).

The geometrical workspace of *BetaBot* is only limited by the maximum and minimum lengths of the spine assuming that there are no limitations on the cables' lengths and therefore, the shape of the workspace is a half sphere above the base whose radius is determined by the maximum length of the spine. It is clear that there is no possibility of any interference between the cables because of the non-rotating motion of the end-effector.
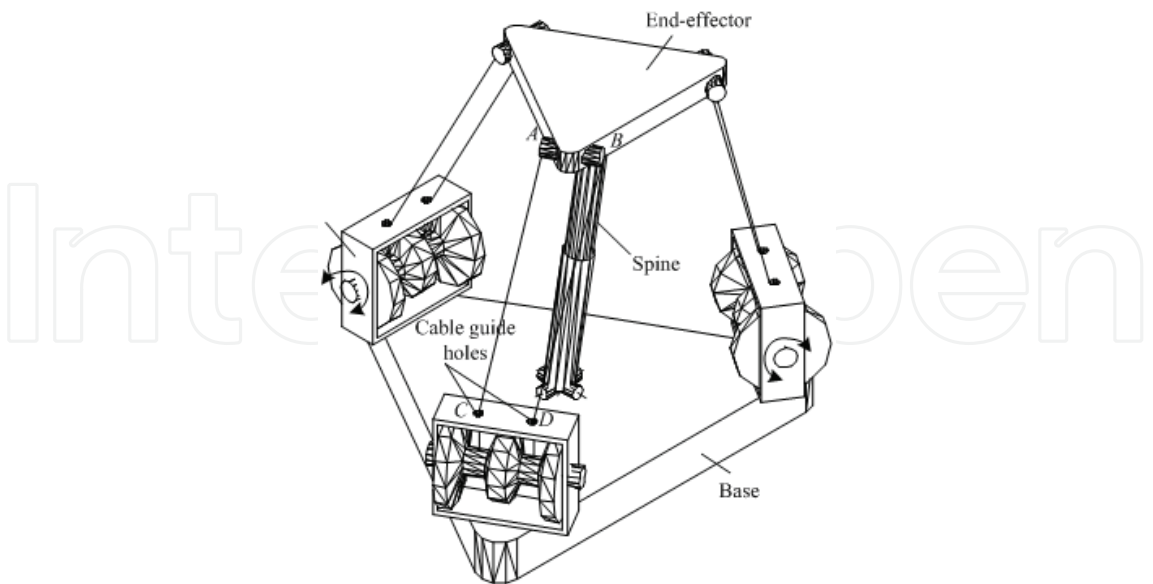
Figure 2. *BetaBot*: a 3 DoF cable-based manipulator with pure translational motion

4.1 Tensionability of *BetaBot*

BetaBot is tensionable everywhere in its workspace providing that certain conditions are enforced on the geometry of the manipulator as illustrated in Fig. 3:

Condition 1. End-effector has a triangular shape as shown in Fig. 3. Each pair of the parallel cables is attached to one edge of the triangle,

Condition 2. The guide holes on the winch frames are all on the same plane and form a triangle called Base triangle. This triangle is similar (and parallel) to the triangle of the end-effector but larger. As a result, the end-effector along with the cables form a convex region or a polyhedral

Condition 3. Any two cables never become in-line

Condition 4. The connection points of the spine, O and O' in Fig. 3, are on the base and end-effector triangles, respectively and have the same trilinear coordinates[2]. A direct result is that the spine never intersects with the faces of the polyhedral of Condition 2 (even if the spine and cables are extended from the base side).

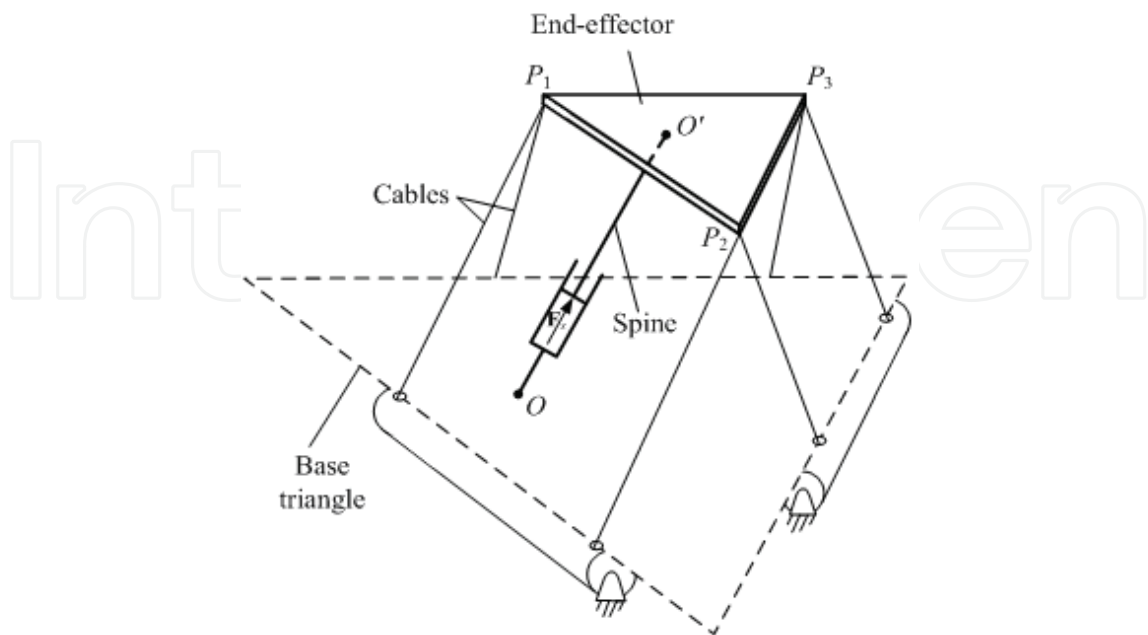[2] The ratio between their distances from the triangle vertices are the same

Figure 3. The prefered geometry of BetaBot which guarantees its tensionability

To prove the tensionability, we use the theorem given in the last section. Therefore, for *BetaBot* to be tensionable, an arbitrary positive spine force should be balanced by positive cable tensions. For the proof, a geometrical approach is employed which shows that the solution of static equilibrium equations consists of a set of positive tensions. Since the proof is lengthy, it is presented by four lemmas and one theorem.

Lemma 1.
If *BetaBot* meets the above mentioned conditions, then the three planes each of which formed by one pair of parallel cables intersect at one point such as R (see Fig. 4).

Proof.
In Fig. 4, consider the plane that includes P_1, P_2, B_1 and B_2: If B_1P_1 and B_2P_2 are extended, they meet at a point called R and form triangle ΔB_1RB_2 (otherwise they will be parallel which implies the end-effector and the base triangle are equal contradicting Condition 2). In this triangle we have:

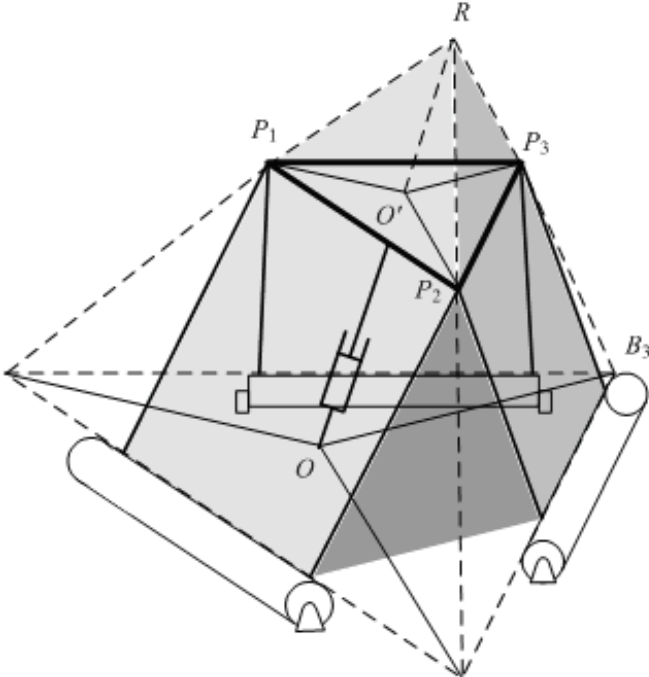$$P_1P_2 \| B_1B_2 \Rightarrow \frac{RP_2}{RB_2} = \frac{P_1P_2}{B_1B_2} \tag{8}$$

Figure 4. The three planes formed by parallel cables and the spine meet at a point called R.

Now, consider the second plane that includes P_2, P_3, B_2 and B_3: If B_2P_2 and B_3P_3 are extended, they meet at a point called R'. Note that R' and R are both on the line of P_2B_2. In triangle $\Delta B_2 R' B_3$ we have:

$$P_2P_3 \| B_2B_3 \Rightarrow \frac{R'P_2}{R'B_2} = \frac{P_2P_3}{B_2B_3} \tag{9}$$

Also, we know from Condition 2 that $\Delta P_1P_2P_3$ is similar to $\Delta B_1B_2B_3$ and hence:

$$\frac{P_1P_2}{B_1B_2} = \frac{P_2P_3}{B_2B_3} \tag{10}$$

which, by considering Eqs. (8, 9), results in:

$$\frac{R'P_2}{R'B_2} = \frac{RP_2}{RB_2} \tag{11}$$

Considering that R and R' are on the same line, Eq. (11) states that R and R' are coincident and a similar reasoning shows that the third plane also passes through R.

Lemma 2.
In *BetaBot*, the direction of the spine passes through point R as found in Lemma 1.

Proof.
Assume point R, as given in Fig. 4, is connected to O' and extended to intersect the base at point O'' (not shown in the figure). It is needed to show that O'' coincides with O. This is shown by the following relations:

$$\Delta RO''B_1: \quad O'P_1 \| O''B_1 \quad \Rightarrow \quad \frac{O'P_1}{O''B_1} = \frac{RP_1}{RB_1} \tag{12}$$

$$\Delta RB_1B_2: \quad P_1P_2 \| B_1B_2 \quad \Rightarrow \quad \frac{RP_1}{RB_1} = \frac{RP_2}{RB_2} \tag{13}$$

$$\Delta RO''B_2: \quad O'P_2 \| O''B_2 \quad \Rightarrow \quad \frac{O'P_2}{O''B_2} = \frac{RP_2}{RB_2} \tag{14}$$

As a result:

$$\frac{O'P_1}{O''B_1} = \frac{RP_1}{RB_1} = \frac{RP_2}{RB_2} = \frac{O'P_2}{O''B_2} \tag{15}$$

and using a similar approach on $\Delta R O'' B_3$, ΔRB_1B_3 and $\Delta R O'' B_1$, we have:

$$\frac{O'P_1}{O''B_1} = \frac{RP_1}{RB_1} = \frac{RP_3}{RB_3} = \frac{O'P_3}{O''B_3} \tag{16}$$

which results in:

$$\frac{O'P_1}{O''B_1} = \frac{O'P_2}{O''B_2} = \frac{O'P_3}{O''B_3} \tag{17}$$

However, Condition 4 states that:

$$\frac{O'P_1}{OB_1} = \frac{O'P_2}{OB_2} = \frac{O'P_3}{OB_3} \tag{18}$$

By comparing Eqs. (17) and (18), it is concluded that O' coincides with O''.

For the next two lemmas, Fig. 5 is used. In Fig. 5a, the region bounded by the cables is the polyhedral of Condition 2. The faces of this polyhedral are formed by the cables. This polyhedral has six faces S_{ij} (i,j=1,2,3 and $i<j$) each of which formed by two cable directions: $\hat{\mathbf{u}}_i$ and $\hat{\mathbf{u}}_j$. In Fig. 5b, the force diagram of the end-effector is shown. $\mathbf{F}_s$ is the spine force and each force vector $\sigma_i \hat{\mathbf{u}}_i$ represents the force of two parallel cables and hence σ_i is the total tension of the two parallel cables along $\hat{\mathbf{u}}_i$. Now, the next two lemmas follow.

Figure 5. a) The polyhedra formed by the cables in *BetaBot* b) The cone of the cable forces

Lemma 3.

According to Fig. 5a, the half line Rl which starts from R in the direction of $\hat{\mathbf{u}}_1$ intersects line segment P_1P_2 at E.

Proof.

It is obvious that half line Rl intersects the line of P_1P_2 otherwise, they should be in parallel which implies that the first pair of cables are in-line contradicting Condition 3. The major effort of this proof is to show that the intersection occurs between P_1 and P_2, i.e. $E \in P_1P_2$. For the proof, it is sufficient to show that E belongs to the polyhedral of Fig. 5a. Let $\mathbf{E}$ be the position vector of E with respect to $OXYZ$ reference frame. It is known that:

$$\mathbf{E} = \mathbf{R} + \alpha\hat{\mathbf{u}}_1 \tag{19}$$

where $\mathbf{R}$ is the position vector of R and a is a positive real number. The polyhedral of Fig. 5a is represented as a set of points in the Cartesian space by:

$$\mathbf{\Phi} = \left\{ \phi \in \mathsf{R}^3 \,\middle|\, \hat{\mathbf{n}}_{ij} \cdot \mathbf{\varphi} \le d_{ij} \quad i,j = 1,2,3 \, i \le j \right\} \tag{20}$$

where the center of coordinate O is set to be inside the polyhedral, $\hat{\mathbf{n}}_{ij}$ is the unit vector normal to face S_{ij} pointing outward the polyhedral, and d_{ij} is the distance between face S_{ij} and the center of coordinates O.

In order to have $E \in \mathbf{\Phi}$, the following six inequalities should be satisfied:

$$\hat{\mathbf{n}}_{ij} \cdot \mathbf{E} \le d_{ij} \quad i,j = 1,2,3 \quad i \le j \tag{21}$$

For $i=j=1$, we have:

$$\begin{aligned} \hat{\mathbf{n}}_{11} \cdot \mathbf{E} &= \hat{\mathbf{n}}_{11} \cdot \left(\mathbf{R} + \alpha\hat{\mathbf{u}}_1\right) \\ &= \hat{\mathbf{n}}_{11} \cdot \mathbf{R} + \alpha\hat{\mathbf{m}}_{11} \cdot \hat{\mathbf{u}}_1 \end{aligned} \tag{22}$$

since $R \in S_{11}$ and $\hat{\mathbf{n}}_{11} \cdot \hat{\mathbf{u}}_1 = 0$, it is concluded that $\hat{\mathbf{n}}_{11} \cdot \mathbf{E} = d_{11} \le d_{11}$.

For $i=j=2$, we have:

$$\begin{aligned} \hat{\mathbf{n}}_{22} \cdot \mathbf{E} &= \hat{\mathbf{n}}_{22} \cdot \left(\mathbf{R} + \alpha\hat{\mathbf{u}}_1\right) \\ &= \hat{\mathbf{n}}_{22} \cdot \mathbf{R} + \alpha\hat{\mathbf{m}}_{22} \cdot \hat{\mathbf{u}}_1 \end{aligned} \tag{23}$$

it is known that $R \in S_{22}$ hence, we have:

$$\hat{\mathbf{n}}_{22} \cdot \mathbf{E} = d_{22} + \alpha\hat{\mathbf{m}}_{22} \cdot \hat{\mathbf{u}}_1 \overset{?}{\le} d_{22} \tag{24}$$

which requires $\alpha\hat{\mathbf{n}}_{22} \cdot \hat{\mathbf{u}}_1 \le 0$. To show this, an auxiliary point with position vector $\mathbf{P}_2 + \alpha\hat{\mathbf{u}}_1$ is considered. This point is on cable 2 according to Fig. 5a and hence belongs to polyhedral $\mathbf{\Phi}$. Therefore, one of the inequalities that this point should satisfy is:

$$\hat{\mathbf{n}}_{22} \cdot \left(\mathbf{P}_2 + \alpha\hat{\mathbf{u}}_1\right) \le d_{22} \tag{25}$$

P_2 is a vertex of the end-effector triangle and thus, $P_2 \in S_{22}$ which implies that

$\hat{n}_{22} \cdot P_2 = d_{22}$. Using this in Eq. (25) results:

$$\hat{\mathbf{n}}_{22} \cdot \left(\mathbf{P}_2 + \alpha \hat{\mathbf{u}}_1\right) = d_{22} + \alpha \hat{\mathbf{n}}_{22} \cdot \hat{\mathbf{u}}_1 \leq d_{22}$$
$$\Rightarrow \alpha \hat{\mathbf{n}}_{22} \cdot \hat{\mathbf{u}}_1 \leq 0 \qquad (26)$$

which was needed to satisfy inequality (24). Similar proof is used for $i=j=3$, by taking $\mathbf{P}_1 + \alpha \hat{\mathbf{u}}_1$ as the auxiliary point.
For $i=1$ and $j=2$, the inequality to be satisfied is:

$$\hat{\mathbf{n}}_{12} \cdot \mathbf{E} \leq d_{12}$$
$$\text{or} \quad \hat{\mathbf{n}}_{12} \cdot \left(\mathbf{R} + \alpha \hat{\mathbf{u}}_1\right) \leq d_{12} \qquad (27)$$
$$\text{or} \quad \hat{\mathbf{n}}_{12} \cdot \mathbf{R} + \alpha \hat{\mathbf{n}}_{12} \hat{\mathbf{u}}_1 \leq d_{12}$$

Again, since $R \in \mathbf{\Phi}$, we have $\hat{\mathbf{n}}_{12} \cdot \mathbf{R} \leq d_{12}$. Therefore for inequality (27) to hold true, it is sufficient to show that $\alpha \hat{\mathbf{n}}_{12} \hat{\mathbf{u}}_1 = 0$ which is obvious because $\hat{\mathbf{u}}_1$ is normal to $\hat{\mathbf{n}}_{12}$. A similar approach works for $i=1$, $j=3$. Finally, for $i=2$, $j=3$, we should have:

$$\hat{\mathbf{n}}_{23} \cdot \mathbf{E} = \hat{\mathbf{n}}_{23} \cdot \left(\mathbf{R} + \alpha \hat{\mathbf{u}}_1\right) \leq d_{23} \qquad (28)$$

Again, we have $R \in \mathbf{\Phi}$ and thus $\hat{\mathbf{n}}_{23} \cdot \mathbf{R} \leq d_{23}$. It would be sufficient to show that $\alpha \hat{\mathbf{n}}_{23} \hat{\mathbf{u}}_1 \leq 0$. For this purpose, consider the cone that is formed by extending S_{12}, S_{13} and S_{23}. This cone has a similar shape to the one of Fig. 5b. The edges of this cone are along $\hat{\mathbf{u}}_1$, $\hat{\mathbf{u}}_2$ and $\hat{\mathbf{u}}_3$. Let the apex of this cone be called W and take $\mathbf{W} + \alpha \hat{\mathbf{u}}_1$ as an auxiliary point which belongs to the cone and hence satisfies the following inequality:

$$\hat{\mathbf{n}}_{23} \cdot \left(\mathbf{W} + \alpha \hat{\mathbf{u}}_1\right) \leq d_{23} \qquad (29)$$

Now, since $\hat{\mathbf{n}}_{23} \cdot \mathbf{W} = d_{23}$, it is concluded that $\alpha \hat{\mathbf{n}}_{23} \hat{\mathbf{u}}_1 \leq 0$ which satisfies inequality (28) and hence $E \in \mathbf{\Phi}$, which completes the proof.

Lemma 4.
According to the force diagram of Fig. 5b, the spine force is balanced by positive σ_i's $i=1, 2, 3$ i.e.:

$$\sigma_1 \hat{\mathbf{u}}_1 + \sigma_2 \hat{\mathbf{u}}_2 + \sigma_3 \hat{\mathbf{u}}_3 = -\mathbf{F}_s \qquad (30)$$

Proof.
We first show that the direction of spine force lies inside the cone formed by cables direction vectors: $\hat{\mathbf{u}}_1$, $\hat{\mathbf{u}}_2$ and $\hat{\mathbf{u}}_3$. For this purpose, we use Condition 4 which states the spine never intersects any faces of the polyhedral of cables (Fig. 5a). Considering that the faces of the cone of Fig. 5b are parallel to S_{12}, S_{13}

and S_{23}, respectively, it is understood that $\mathbf{F}_s$ never touches the faces of the cone and hence, is inside the cone. Based on the definition of a convex cone (Yamaguchi, 2002), the cone of Fig. 5b can be expressed as:

$$\Psi = \left\{ \psi \in \mathsf{R}^3 \middle| \psi = \sigma_1 \hat{\mathbf{u}}_1 + \sigma_2 \hat{\mathbf{u}}_2 + \sigma_3 \hat{\mathbf{u}}_3 \quad \sigma_1, \sigma_2, \sigma_3 \geq 0 \right\} \tag{31}$$

Now, since $\mathbf{F}_s$ is always inside the cone, it can be considered as the position vector for a point inside the cone. As a result, the definition of the cone given in Eq. (31) states that:

$$-\mathbf{F}_s = \sigma_1 \hat{\mathbf{u}}_1 + \sigma_2 \hat{\mathbf{u}}_2 + \sigma_3 \hat{\mathbf{u}}_3 \quad \sigma_1, \sigma_2, \sigma_3 \geq 0 \tag{32}$$

which completes the proof.

Theorem 2.
If *BetaBot* satisfies Conditions 1-4 as explained before, it is tensionable everywhere in its workspace.

Proof.
For the proof, we show that a positive spine force is statically balanced by positive tension in cables. For this purpose, first consider the force equilibrium of the end-effector (see Fig. 5b). According to Lemma 4, the force equilibrium on the end-effector is met by positive σ_1, σ_2 and σ_3, where for instance, σ_1 is the total tension of cables 1 (τ_1) and 2 (τ_2). Now, let:

$$\tau_1 = \frac{P_2 E}{P_1 P_2} \sigma_1 \qquad \tau_2 = \frac{P_1 E}{P_1 P_2} \sigma_1 \tag{33}$$

therefore, we have $\tau_1, \tau_2 > 0$, $\tau_1 + \tau_2 = \sigma_1$. Since E is on $P_1 P_2$ (Lemma 3) and using Eq. (33), the moments of $\tau_1 \hat{\mathbf{u}}_1$ and $\tau_2 \hat{\mathbf{u}}_1$ about E cancel each other. As a result, force vector $\sigma_1 \hat{\mathbf{u}}_1$ applied at E is an equivalent for cable forces $\tau_1 \hat{\mathbf{u}}_1$ and $\tau_2 \hat{\mathbf{u}}_1$. Note that the line of action of this equivalent force passes through R. Similarly, other cable forces can be replaced by equivalent forces whose lines of action pass through R. Now, based on Lemma 2, the direction of the spine also passes through the same point (R) and hence, the equilibrium of the moments is also satisfied which completes the proof.

5. DishBot

DishBot is another spatial cable-based manipulator with translational motion shown in Fig. 6. In *DishBot*, two independent sets of cables are used. The first set, called drive cables, moves the end-effector and the second set, named passive cables, eliminates the rotation. The spine, in this design, is composed of a bar sliding inside a collar along with a spring. The collar is connected to the center of the base by a universal joint. The spring is fixed to the collar from one end and to the bar from the other end. It produces a compressive force to maintain tension in the drive cables. A ball-and-socket is used to connect the end-effector to the spine.

As seen in Fig. 6b, drive cables are connected to the tip of the spine similar to the tripod design of Landsberger (Landsberger & Sheridan, 1985) or Mianowski's robot (Mianowski & Nazarczuk, 1990). Each cable is pulled and collected by a winch that is hinged to the base such that it can align itself with the cable direction.

In Fig. 6c, the passive cables are shown. Each passive cable starts from the end-effector on the top and proceeds down to the base where it bends around a pulley (such as pulley *i* in Fig. 6c) and goes towards the spine. Using another pulley (such as pulley *j*) on the collar to guide the cable, it reaches the bottom end of the spine bar. Each passive cable is in series with a tensile pre-tensioning spring to produce tensile force in the cable.

The length of the passive cables are constant which makes the end-effector stay parallel to the base. However, the perfect parallelness is only obtained if the radii of the two guiding pulleys are zero and the pulleys on the collar coincide with the center of the universal joint.

Fig. 7 shows how the passive cables make the end-effector stay parallel to the base in a similar 2D manipulator. In practice, complete parallelness is not achieved since the pulleys have non-zero radius and they cannot be placed at the center of the universal joint; however, the error can be minimized by proper sizing and positioning of the pulleys.

Assuming the passive cables are always taut and maintain the orientation of the end-effector, the kinematics of *DishBot* is identical to a tripod since it only depends on the drive cables. The inverse and direct kinematics have closed form solutions (Tsai, 1996). The geometrical workspace of *DishBot* is the half sphere above the base whose radius is the maximum length of the spine. Similar to *BetaBot*, the size of the workspace is only limited by the maximum and minimum length of the spine. There is no possibility of interference between the cables and spine as long as:

1. The spine is located inside the cone of drive cables,
2. The cone of drive cables is inside the prism of passive cables.

(a)

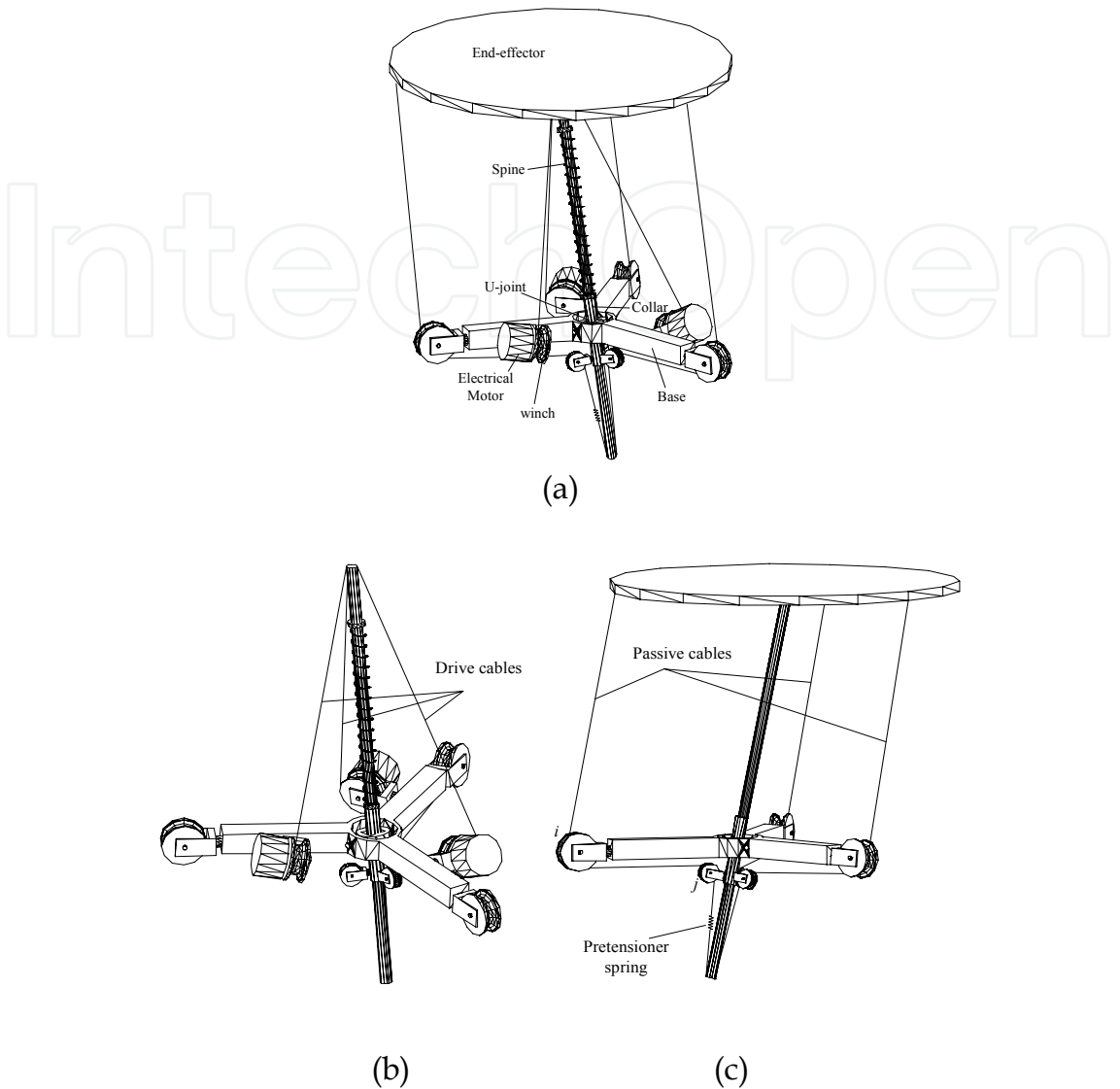(b)   (c)

Figure 6. a) *DishBot*: a 3 DoF translational cable-based manipulator with two independent sets of cables. b) The configuration of the drive cables c) The configuration of the passive cables
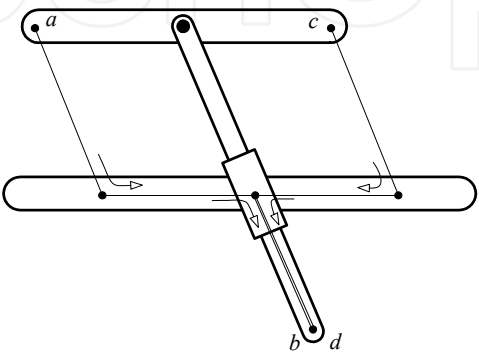

Figure 7. Assuming the lengths of the two cables *ab* and *cd* are equal, the end-effector always remains parallel to the base

5.1 Tensionability of *DishBot*

For the tensionability of *DishBot*, Theorem 1 given in Section 3 is not sufficient. The reason is that the spine force only affects the tension of drive cables and has no influence on the passive ones. As a result, it cannot leverage all the tensions. However, it should be noted that each passive cable has a pre-tensioning spring to maintain the tension. Therefore, the tensionability can be still proved based on its definition in Section 2. For the proof of tensionability, we use the idea of Theorem 1 (not the theorem itself), i.e. tension can be generated in the cables to any extent while the static equilibrium is satisfied.

The free body diagram of the end-effector is shown in Fig. 8. The passive cables are in parallel with the spine and their tensions are shown by a superscript p while for the tension of drive cables, a superscript d is used. The static equilibrium equations are found to be:

$$\sum \mathbf{F} = \tau_1^d \hat{\mathbf{u}}_1 + \tau_2^d \hat{\mathbf{u}}_2 + \tau_3^d \hat{\mathbf{u}}_3 + \left(f_s - \tau_1^d - \tau_2^d - \tau_3^d\right)\hat{\mathbf{w}} = \mathbf{0} \tag{34}$$

$$\sum \mathbf{M} = -\tau_1^p \left(\mathbf{r}_1 \times \hat{\mathbf{w}}\right) - \tau_2^p \left(\mathbf{r}_2 \times \hat{\mathbf{w}}\right)\hat{\mathbf{u}}_1 - \tau_3^p \left(\mathbf{r}_1 \times \hat{\mathbf{w}}\right) = \mathbf{0} \tag{35}$$

where $\tau_i^d \hat{\mathbf{u}}_i$'s are drive cable forces (i=1,2,3), $\tau_j^p \hat{\mathbf{w}}$'s are passive cable forces, $\mathbf{r}_j$'s are the position vectors of the anchor points of the passive cables (j=1,2,3) and $f_s \hat{\mathbf{w}}$ is the spine force.
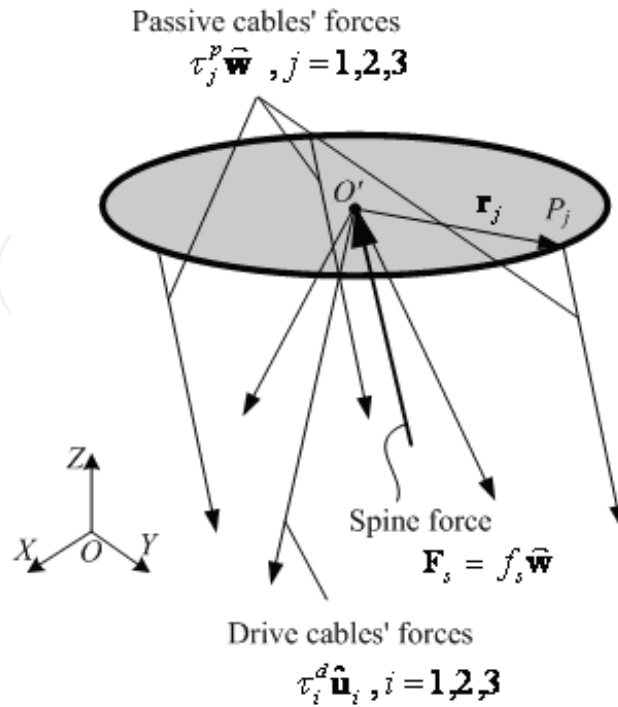

Figure 8. Free body diagram of DishBot's end-effector

A quick inspection of the above equations shows that Eq. (35), which is the equilibrium of the moments, is a set of homogenous equations independent from the spine force which, in general, results in zero tension for passive cables. The tension of the drive cables are found from Eq. (34). Note that the drive cables form a cone which contains the spine and hence, using Lemma 4, the drive cable tensions are positive as long as the equivalent spine force, $f_s - \tau_1^p - \tau_2^p - \tau_3^p$, is positive (compressive). As a conclusion, tension in the drive cables can be generated to any desired level by choosing a large enough spine force but it does not affect the tension in the passive cables.

In order for *DishBot* to be tensionable, we also need to show that the tension in the passive cables can be increased to any desired level. For this purpose, note that, in Fig. 8, if O' is the geometrical center of the three anchor points of the passive cables (P_1, P_2 and P_3) then Eq. (35) has non-zero solutions for passive cable tensions. In this case, the solution would be $\tau_1^p = \tau_2^p = \tau_3^p = \tau^p$ where τ^p is an arbitrary real value and thus can be positive. It is known that such a geometrical center coincides with the centroid of triangle $\Delta P_1 P_2 P_3$. As a result, if O' is the centroid of triangle $\Delta P_1 P_2 P_3$, positive equal tensions in passive cables are determined only by the pre-tensioning springs.

As a conclusion, *DishBot* is tensionable as long as the following conditions are met:

1. O' is the centroid of $\Delta P_1 P_2 P_3$,
2. The pretension of the pre-tensioning springs are equal (τ^p) and positive (tensile),
3. The spine lies inside the cone of the drive cables.
4. The spine force satisfies $f_s - \tau_1^p - \tau_2^p - \tau_3^p > 0$ which means $f_s > 3\tau^p$.

6. Planar cable-based manipulators with translational motion

Planar manipulators with translational motion (in XY plane) are sufficient for many industrial pick-and-place applications such as packaging and material handling. Simplicity of these manipulators compared to spatial ones further facilitates their applications where a two axis motion is sufficient (Chan, 2005). Two new designs of planar cables-based manipulators with translational motion are studied here that are tensionable everywhere in their workspace.

Schematic diagrams of these manipulators are shown in Fig. 9. The spine is connected to the base and end-effector by revolute joints. The end-effector is constrained by three cables. Two of the cables form a parallelogram which eliminates the rotation of the end-effector as long as the cables are taut. As a result, the end-effector can only move in X and Y directions.
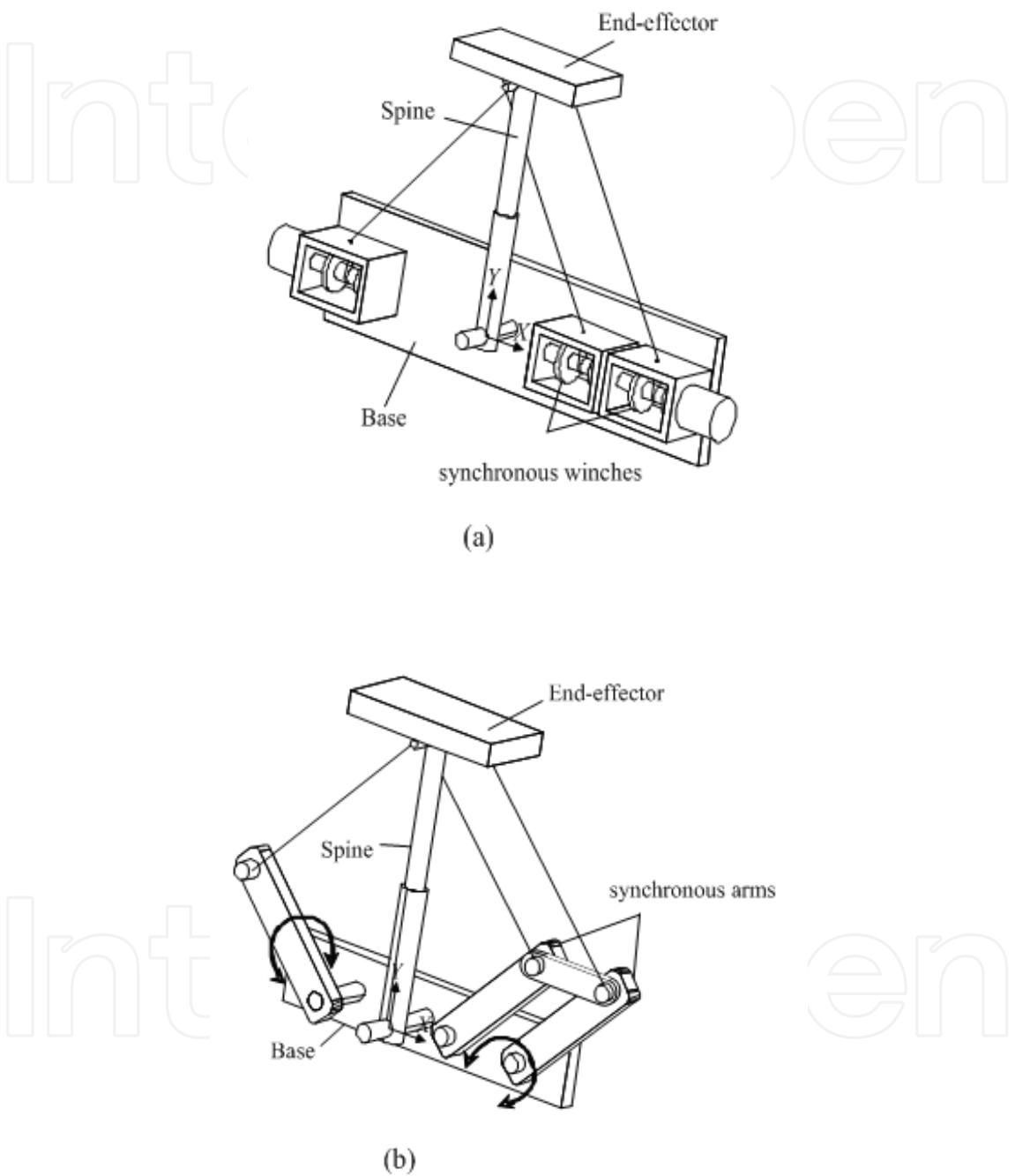
(a)

(b)

Figure 9. Planar cable-based manipulators with pure translational degrees of freedom

In the first design (Fig. 9a), the parallelogram is maintained by two winches with a common shaft which makes them move simultaneously and hence, keep the cable lengths equal. Similar to *BetaBot* and *DishBot*, the workspace of this manipulator is only limited by the minimum and maximum lengths of the

spine and hence it can theoretically span a half circle above the base. In the second design (Fig. 9b), a pair of synchronous rotating arms preserves the parallelogram without changing the length of the cables and therefore, possess a smaller workspace. The synchronization can be obtained by a pair of pulleys and a timing belt or a simple 4-bar parallelogram as seen in Fig. 9b.

The kinematics of these manipulators consist of a single planar cone and hence easy to formulate for both direct and inverse solutions. In this paper, however, our main focus is on the their tensionability and rigidity which is presented in the following.

6.1 Tensionability of Planar Manipulators

The planar manipulators of Fig. 9 are both tensionable everywhere in their workspaces. This can be proved using an approach similar to the one that was used for *BetaBot*. There are two geometrical conditions that should be met for the tensionability of these two manipulators. As depicted in Fig. 10a, these two conditions are as follows:
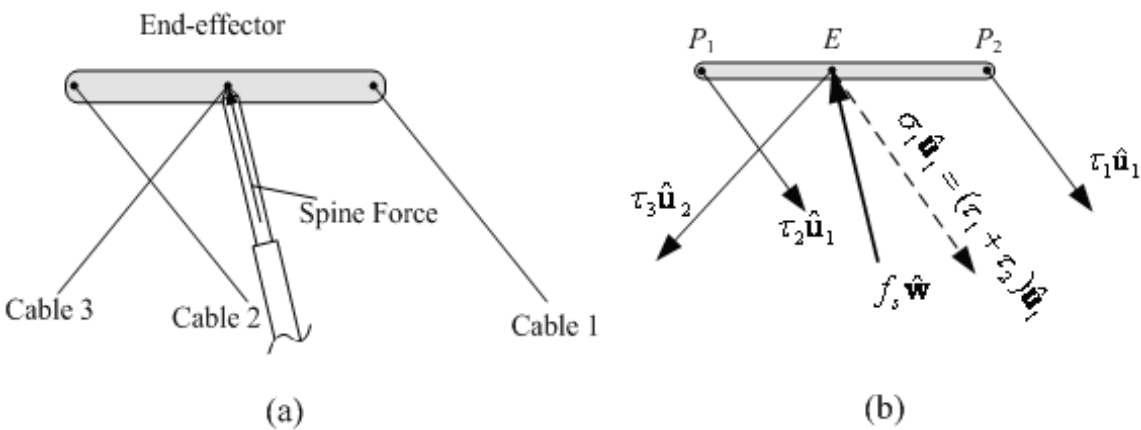

Figure 10. a) The configuration of the cables and spine in planar manipulators, b) The free body diagram of the end-effector

Condition 1.   Cable 1 (Fid. 10a) is always on the right and Cable 3 is always on the left side of the spine. This is obtained if the spine is hinged to the base at a proper point between the two sets of cables.

Condition 2.   On the end-effector, the spine and Cable 3 are concurrent at point E which is located somewhere between Cables 1 and 2.

To prove the tensionability, we show that a compressive spine force can be balanced by positive tensions in the cables. The proof is quite similar to the one of Theorem 2 and is briefly explained here.

We first consider the force equilibrium of the end-effector subject to a compressive spine force. According to the free body diagram shown in Fig. 10b, we have:

$$\sigma_1 \hat{\mathbf{u}}_1 + \tau_3 \hat{\mathbf{u}}_2 + f_s \hat{\mathbf{w}} = \mathbf{0} \quad \Rightarrow \quad \sigma_1 \hat{\mathbf{u}}_1 + \tau_3 \hat{\mathbf{u}}_2 = -f_s \hat{\mathbf{w}} \tag{36}$$

Due to Condition 1, the direction of the spine, $\hat{\mathbf{w}}$ is located between $\hat{\mathbf{u}}_1$ and $\hat{\mathbf{u}}_2$ (cable directions). Therefore, the projection of $-f_s \hat{\mathbf{w}}$ on $\hat{\mathbf{u}}_1$ and $\hat{\mathbf{u}}_2$ will be positive and hence $\sigma_1, \tau_3 > 0$. Now, let:

$$\tau_1 = \frac{P_1 E}{P_1 P_2} \sigma_1 \quad \text{and} \quad \tau_2 = \frac{P_2 E}{P_1 P_2} \sigma_1 \tag{37}$$

It is clear that $\tau_1 + \tau_2 = \sigma_1$. Since $\sigma_1 > 0$ and due to the distribution given in Eq. (37), the moment of $\tau_1 \hat{\mathbf{u}}_1$ about E cancels the one of $\tau_2 \hat{\mathbf{u}}_1$ and hence, these two forces can be replaced by $\sigma_1 \hat{\mathbf{u}}_1$ without violating the static equilibrium. Finally, since all three forces on the end-effector, $\sigma_1 \hat{\mathbf{u}}_1$, $\tau_1 \hat{\mathbf{u}}_1$ and $\tau_2 \hat{\mathbf{u}}_1$, are concurrent at E, the equilibrium of the moments is also met which completes the proof.

7. Conclusion

In this paper, several new cable-based manipulators with pure translational motion were introduced and their rigidity where thoroughly studied. The significance of these new designs can be summarized in two major advantages over the other cable-based manipulators:

1. Cables are utilized to provide kinematic constraints to eliminate rotational motion of the end-effector. In many industrial applications, reduced DoF manipulators are sufficient to do the job at a lower cost (less number of axes).

2. These manipulators can be rigidified everywhere in their workspace using a sufficiently large pretension in the cables.

In order to study the rigidity of these manipulators, the concept of tensionability was used and a theorem was given to provide a sufficient condition for tensionability. Using this theorem, tensionability of each manipulator was proved

using line geometry and static equilibrium in vector form. For each of these manipulators, it was shown that as long as certain conditions are met by the geometry of the manipulator, the tensionable workspace in which the manipulator can be rigidified, is identical to the geometrical workspace found from the kinematic analysis.

BetaBot and the planar manipulators are tensionable everywhere and can be rigidified only by a sufficiently large spine force. In *DishBot*, on top of the geometrical conditions, a relation between the spine force and pre-tensioning springs of passive cables should be also satisfied to maintain the rigidity of the manipulator.

8. References

Barrette G.; Gosselin C. (2005), Determination of the dynamic workspace of cable-   driven planar parallel mechanisms, *Journal of Mechanical Design*, Vol. 127, No.   3, pp. 242-248

Behzadipour S. (2005), *High-speed Cable-based Robots with Translational Motion*, PhD   Thesis, University of Waterloo, Waterloo, ON, Canada

Behzadipour S.; Khajepour A., (2006), Stiffness of Cable-based Parallel Manipulators   with Application to the Stability Analysis, *ASME Journal of Mechanical Design*,   Vol. 128, No. 1, 303-310

Chan E. (2005), *Design and Implementation of a High Speed Cable-Based Planar Parallel Manipulator*, MASc Thesis, University of Waterloo, Waterloo, ON, Canada.

Clavel R., (1991), *Conception d'un robot parallele rapide a 4 degres deliberate*, PhD Thesis, EPFL, Lausanne

Dekker R. & Khajepour A. & Behzadipour S. (2006), Design and Testing of an Ultra   High-Speed Cable Robot", *Journal of Robotics and Automation*, Vol. 21, No. 1,   pp. 25-34

Ferraresi C.; Paoloni M.; Pastorelli S.; Pescarmona F, (2004), A new 6-DOF parallel   robotic structure actuated by wires: the WiRo-6.3, *Journal of Robotics Systems*,   Vol. 21, No. 11, pp. 581-595

Gallina P; Rosati G., (2002), Manipulability of a planar wire driven haptic device,   *Mechanism and Machine Theory*, Vol. 37, pp. 215-228

Gouttefarde M.; Gosselin C. (2006), Analysis of the wrench-closure workspace of   planar parallel cable-driven mechanisms, *IEEE Transactions on Robotics*, Vol.   22, No. 3, pp. 434-445

Kawamura S.; Choe W.; Tanak S. Pandian S.R., (1995),Development of an ultrahigh speed robot FALCON usign wire driven systems, *Proceedings of IEEE   International Conference on Robotics and Automation*, pp. 215-220, IEEE, 1995

Khajepour A. & Behzadipour S. & Dekker R. & Chan E. (2003), Light Weight Parallel Manipulators Using Active/Passive Cables, *US patent provisional file No. 10/615,595*

Landsberger S.E.; Sheridan T.B., (1985), A new design for parallel link manipulators, *Proceedings of the International Conference on Cybernetics and Society*, pp. 81-88, Tuscon AZ, 1985

Landsberger S.E.; Shanmugasundram P. (1992), Workspace of a Parallel Link Crane, *Proceedings of IMACS/SICE International Symposium on Robotics, Mechatronics and Manufacturing Systems*, pp. 479-486, 1992

Ming A.; Higuchi T. (1994a), Study on multiple degree-of-freedom positioning mechanism using wires (Part1), *International Journal of Japan Society of Precision Engineering*, Vol. 28, No. 2, pp. 131-138

Ming A.; Higuchi T. (1994b), Study on multiple degree-of-freedom positioning mechanism using wires (Part2), *International Journal of Japan Society of Precision Engineering*, Vol. 28, No. 3, pp. 235-242

Ogahara Y.; Kawato Y.; Takemura K.; Naeno T., (2003), A wire-driven miniature five fingered robot hand using elastic elements as joints, *Proceedings of IEEE/RSJ International Conference on Intelligent Robots and Systems*, pp. 2672-2677, Las Vegas, Nevada, 2003

Oh s.; Makala K. K.; Agrawal S., (2005a) Dynamic modeling and robust controller design of a two-stage parallel cable robot, *Multibody System Dynamics*, Vol. 13, No. 4, pp. 385-399

Oh s.; Makala K. K.; Agrawal S., Albus J. S. (2005b), A dual-stage planar cable robot: Dynamic modeling and design of a robust controller with positive inputs, *ASME Journal of Mechanical Design*, Vol. 127, No. 4, pp. 612-620

Pusey j.; Fattah A.; Agrawal S.; Messina E., (2004), Design and workspace analysis of a 6-6 cable-suspended parallel robot, *Mechanisms and Machine Theory*, Vol. 39, No. 7, pp. 761-778

Robers G.R; Graham T.; Lippitt T. (1998), On the inverse kinematics, statics, and fault tolerance of cable-suspended robots, *Journal of Robotic Systems*, Vol. 15, No. 10, pp. 581-597

Stump E.; Kumar V., (2006), Workspace of cable-actuated parallel manipulators, *ASME Journal of Mechanical Design*, Vol. 128, No. 1, pp. 159-167

Tadokoro S.; Nishioka S.; Kimura T. (1996), On fundamental design of wire configurations of wire-driven parallel manipulators with redundancy, *ASME Proceeding of Japan/USA Symposium on Flexible Automation*, pp. 151-158

Tsai L-W., (1996), Kinematics of A Three DOF Platform With Three Extensible Limbs, In *Recent Advances in Robot Kinematics*, Lenarcic J. and Parenti-Castelli V., pp. 401-410, Kluwer Academic, Netherlands

Verhoeven R.; Hiller M.; Tadokoro S. (1998), Workspace, stiffness, singularities
and   classification of tendon-driven stewart platforms, In *Advances in
Robot   Kinematics Analysis and Control*, Lenarcic J. and Husty L., pp. 105-
114, Kluwer   Academic, Netherlands

Verhoeven R.; Hiller M. (2000), Estimating the controllable workspace of ten-
don-   based Stewart platforms, In *Advances in Robot Kinematics*, Lenarcic
J. and   Stanisic M., pp. 277-284, Kluwer Academic, Netherlands

Yamaguchi F., (2002), *A Totally Four-dimensional Approach / Computer-Aided
Geometric   Design*, Springer-Verlag, Tokyo

Industrial Robotics: Theory, Modelling and Control

Edited by Sam Cubero

This book covers a wide range of topics relating to advanced industrial robotics, sensors and automation technologies. Although being highly technical and complex in nature, the papers presented in this book represent some of the latest cutting edge technologies and advancements in industrial robotics technology. This book covers topics such as networking, properties of manipulators, forward and inverse robot arm kinematics, motion path-planning, machine vision and many other practical topics too numerous to list here. The authors and editor of this book wish to inspire people, especially young ones, to get involved with robotic and mechatronic engineering technology and to develop new and exciting practical applications, perhaps using the ideas and concepts presented herein.

How to reference

In order to correctly reference this scholarly work, feel free to copy and paste the following:

INTECH

open science | open minds